

# Estimated changes in flood quantiles of the river Meuse from resampling of regional climate model output

Robert Leander, T. Adri Buishand and Marcel J. M. De Wit

*Royal Netherlands Meteorological Institute (KNMI), PO Box 201,  
3730 AE De Bilt, The Netherlands*

---

## Abstract

Precipitation and temperature data from three regional climate model (RCM) experiments were used to assess the effect of climatic change on the flood quantiles of the French-Belgian river Meuse. In two of these experiments the RCM was driven by the global atmospheric model HadAM3H of the Hadley Centre (HC), and in the other experiment the RCM was driven by the global coupled atmosphere-ocean model ECHAM4/OPYC3 of the Max-Planck Institute for Meteorology (MPI). RCM simulations for the control climate (1961-1990) and the SRES-scenario A2 (2071-2100) were available. The HBV rainfall-runoff model was used to simulate river discharges. Long synthetic sequences of precipitation and temperature were resampled from the RCM output using a Nearest-Neighbour technique to obtain the flood quantiles for long return periods. The maxima of 10-day precipitation and discharge for the winter half-year (flooding season) were analysed. It was found that the changes in the extreme quantiles of 10-day precipitation and discharge were highly sensitive to the driving GCM. In the runs driven by HC, there was little change in the most extreme quantiles, whereas the MPI-driven run projected a remarkable increase. It is shown that this difference between the HC- and MPI-driven runs is strongly related to the change in the coefficient of variation of the 10-day precipitation amounts, which decreases in the former and hardly changes in the latter. The relevance of bias correction of RCM output with regard to the estimated changes of flood quantiles is demonstrated.

*Key words:* Meuse basin; Regional climate models; Stochastic precipitation modelling; Hydrological modelling; Extreme values; Climatic change

---

---

*Email address:* `leander@knmi.nl` (Robert Leander).

*Preprint submitted to Journal of Hydrology*

# 1 Introduction

2 From the perspective of policy making the interest in the impacts of local cli-  
3 matic change on river flows is increasing. It is generally believed that climate  
4 change will give rise to increased flooding (Kay et al., 2006). For the Nether-  
5 lands potential changes in the statistics of extreme flows are highly relevant,  
6 since the major part of the country is situated in the delta of the rivers Rhine  
7 and Meuse.

8 Most of the research on the impact of climate change on river discharges in the  
9 Netherlands relates to the river Rhine. Kwadijk and Rotmans (1995) applied  
10 change fields based on seven equilibrium experiments with general circulation  
11 models (GCMs) to the observed monthly precipitation and temperature and  
12 used the perturbed data to drive a distributed hydrological model (RHINE-  
13 FLOW) for the river basin. The same approach was followed in a study co-  
14 ordinated by the International Commission for the Hydrology of the Rhine  
15 Basin (CHR) using the output from one transient and two equilibrium GCM  
16 experiments (Grabs, 1997). Similar to Kwadijk and Rotmans (1995), the ef-  
17 fect of climate change was calculated by applying the changes found in the  
18 GCM experiments to the base-line climate. The assessment of the changes in  
19 river discharges was limited to the mean annual discharge cycle at different  
20 locations in the Rhine basin. In a later study (Middelkoop, 2000) the RHINE-  
21 FLOW model was operated at a temporal resolution of ten days, using data  
22 from the UKHI GCM of the Hadley Centre of the UK Met Office. Shabalova  
23 et al. (2003) were the first to use data from a regional climate model (RCM)  
24 to assess the impact of climate change on the discharges of the river Rhine in  
25 the Netherlands. They used HadRM2 of the Hadley Centre nested within the  
26 global coupled climate model HadCM2. The changes in 10-day precipitation  
27 and temperature were applied to the observed base-line series. It was found  
28 that the changes in extreme flows were very sensitive to the type of transforma-  
29 tion (linear or nonlinear) applied to the precipitation amounts. Lenderink et al.  
30 (2006) investigated the direct use of bias-corrected 10-day HadRM3H regional  
31 climate model data (also from the Hadley Centre) as input to RHINEFLOW.  
32 They compared the changes in discharge with those obtained by perturbing  
33 the RCM control run. One of their findings was that direct use of RCM data  
34 should be preferred, if other discharge characteristics than the mean (such as  
35 extremes) are of interest.

36 For the Meuse basin an extensive study has been carried out by Booij (2002,  
37 2005). He used a first order Markov chain to generate a time series of daily  
38 basin-average precipitation and developed a discrete random cascade model  
39 for spatial disaggregation of precipitation. The parameters of the Markov chain  
40 for the current and the future climate were obtained from transient runs of  
41 three GCMs (CGCM1, HadCM3 and CSIRO9) and two RCMs (HadRM2 and

1 HIRHAM4). The parameters for the cascade model were estimated from the  
2 two RCMs. The semi-distributed HBV model (Lindström et al., 1997) was  
3 used for the hydrological simulations. A subdivision of the Meuse basin into  
4 15 subbasins was compared with a subdivision into 118 subbasins and no  
5 subdivision. De Wit et al. (2006) analysed the impact of climate change on  
6 the occurrence of low flows in the river Meuse, using RCM simulations from the  
7 EU-funded PRUDENCE (Prediction of Regional scenarios and Uncertainties  
8 for Defining European Climate change risks and Effects) project, see e.g.  
9 Christensen and Christensen (2007). Their study indicates that climate change  
10 will lead to a decrease in the average discharge of the Meuse during the low flow  
11 season. Considerable problems were, however, encountered with the simulation  
12 of critical low flow conditions of the Meuse.

13 Leander and Buishand (2007), from here LB07, presented a detailed study  
14 of bias correction of RCM output for the Meuse basin. They also applied  
15 Nearest-Neighbour resampling to obtain long sequences of daily precipitation  
16 and temperature required to simulate long-duration series of river flows. The  
17 study was restricted to the control climate of two experiments with the KNMI  
18 regional climate model RACMO. The simulated series were successfully used  
19 to estimate flood quantiles for return periods far beyond the extent of the  
20 original RCM runs. Therefore, this approach offers a possibility to estimate  
21 extreme flood quantiles for a future climate using data from scenario runs.

22 This paper deals with the estimation of the flood quantiles for the river Meuse  
23 in possible future climate conditions and is a continuation of the work pre-  
24 sented in LB07. Three RCM-GCM configurations are considered. Since for  
25 rivers like the Meuse the occurrence of extreme flows depends strongly on the  
26 variability and the extremes of multi-day precipitation amounts (Tu (2006)  
27 mentions durations between seven and ten days), the statistics of 10-day pre-  
28 cipitation amounts receive much attention.

29 First, a description of the study area is given and the RCM-GCM configura-  
30 tions, the Nearest-Neighbour resampling scheme and the rainfall-runoff model  
31 are discussed. This is followed by an explanation of the bias correction of  
32 RCM output and its implications for the three RCM-GCM configurations.  
33 Then the changes in precipitation and temperature characteristics, found by  
34 comparing the control and scenario runs, are discussed with particular atten-  
35 tion to the quantiles of extreme 10-day precipitation amounts. Subsequently,  
36 the simulated changes of flood quantiles resulting from the hydrological simu-  
37 lations are presented. Finally, the results are summarized and some concluding  
38 remarks are made.

## 1 2 Study area, the used models and methods

2 The river Meuse is the second largest river in the Netherlands. It originates  
3 in the north-east of France and traverses the Belgian Ardennes, which is the  
4 source of a major portion of its discharge. The gauging station Borgharen, con-  
5 sidered in this study, is located near the Belgian-Netherlands border (drainage  
6 area  $\approx 21\,000\text{ km}^2$ ). The mean discharge at this gauging station ranges from  
7  $100\text{ m}^3\text{s}^{-1}$  in September to about  $500\text{ m}^3\text{s}^{-1}$  in January. This strong seasonal  
8 cycle can mainly be ascribed to that of the evapotranspiration (de Wit et al.,  
9 2006).

10 For 15 subbasins the daily area-average precipitation was available for the  
11 historical period 1961-1998. These data were obtained from the Royal Mete-  
12 orological Institute of Belgium for the Belgian subbasins and calculated from  
13 station data (63 stations) for the French subbasins. Daily potential evapo-  
14 ration (PET) data were available for the Belgian subbasins for the period  
15 1967-1998. The PET values for the French subbasins were set equal to the  
16 average over the Belgian part of the basin. Daily temperature was available  
17 for 11 stations in and around the Meuse basin.

18 Three different configurations of an RCM and a GCM are considered in this  
19 study. One consists of the regional climate model RACMO of KNMI, driven by  
20 the high-resolution global atmospheric model HadAM3H (Jones et al., 2001) of  
21 the Hadley Centre. In the other two configurations the regional climate model  
22 RCAO (Räisänen et al., 2004) of the Swedish Meteorological and Hydrolog-  
23 ical Institute (SMHI) was used, either coupled to HadAM3H or the global  
24 atmosphere-ocean model ECHAM4/OPYC3 of the Max-Planck-Institute of  
25 Meteorology (MPI) in Hamburg, Germany (Roeckner et al., 1999). For brevity,  
26 these model configurations are from here denoted as RACMO-HC, RCAO-HC  
27 and RCAO-MPI, respectively.

28 The specific choice of RCM runs and driving GCMs enables us to distinguish  
29 between effects related to the driving GCM and those produced by the RCM  
30 itself. For each configuration two runs were considered, one for the control pe-  
31 riod 1961-1990 and one for the period 2071-2100, based on the SRES-scenario  
32 A2. These RCM runs were performed in the framework of the PRUDENCE  
33 project (Jacob et al., 2007). RCAO and RACMO have a resolution of  $\approx 50$   
34  $\text{km}\times 50\text{ km}$  over the Meuse basin, which is located near the centre of their  
35 domains. From both models 15 grid boxes, displayed in Fig. 1, were selected  
36 which almost entirely cover the basin.

37 The current study is aimed at the investigation of rare events, with return  
38 periods in the order of 1000 years. Since the model runs all have a length of  
39 only 30 years, strong extrapolation would be required, which introduces large

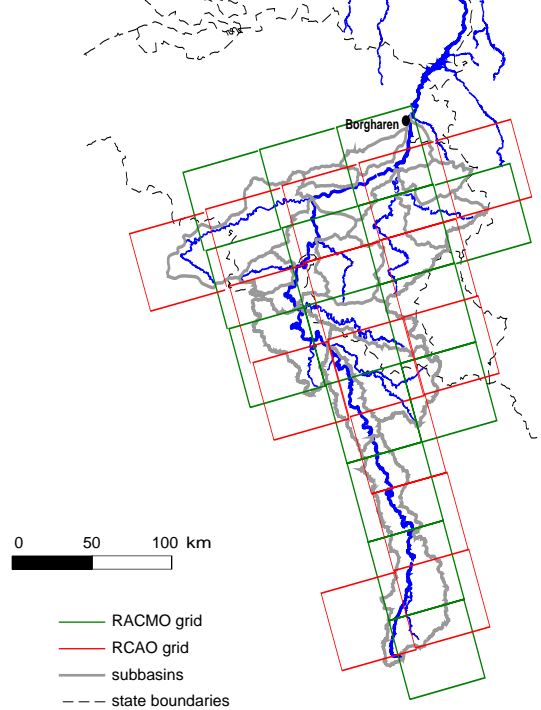


Fig. 1. Locations of the 15 used grid boxes of RACMO (green) and those of RCAO (red), relative to the Meuse subbasins (grey).

1 uncertainties in precipitation and flood quantiles to be estimated. Therefore, a  
 2 data-driven weather generator was used in this study to generate long-duration  
 3 time series of precipitation and temperature. This weather generator is based  
 4 on nearest-neighbour resampling and uses precipitation and temperature data  
 5 from the model simulations (Leander et al., 2005). The algorithm implemented  
 6 for this study essentially samples days from the model runs with replacement.  
 7 The selection of a day being added to the synthetic sequences is conditioned  
 8 on the spatially averaged standardized precipitation and temperature of the  
 9 last added day and the precipitation total of its five predecessors. The general  
 10 principles of nearest-neighbour resampling and the application to daily pre-  
 11 cipitation and temperature are described in Rajagopalan and Lall (1999). One  
 12 of the features of the algorithm is that it is capable of reproducing the daily  
 13 variability and persistence in the underlying data, and hence the variability of  
 14 multi-day aggregates. Therefore, it is a particularly suitable tool in the study  
 15 of extreme discharges. More on the specific implementation of the algorithm  
 16 used in this study can be found in LB07 and Leander et al. (2005).

17 For rainfall-runoff modelling the semi-distributed HBV model, developed at  
 18 SMHI, was used (Lindström et al., 1997). The Meuse basin upstream of Borgharen  
 19 was divided into 15 subbasins, depicted in Fig. 1. Besides daily precipitation  
 20 and temperature, the HBV model also requires daily values of the potential  
 21 evapotranspiration (PET) for each subbasin. In the simulations with observed  
 22 meteorological data the available observed PET values were used. For the sim-  
 23 ulations with RCM data, daily PET was derived from the bias-corrected daily

1 temperature  $T$  using the relation:

$$PET = [1 + \alpha_m(T - \overline{T}_m)]\overline{PET}_m, \quad (1)$$

2 with  $\overline{T}_m$  the mean observed temperature ( $^{\circ}\text{C}$ ) and  $\overline{PET}_m$  the mean observed  
3 PET ( $\text{mm day}^{-1}$ ) for calendar month  $m$  in the period 1967-1998. The propor-  
4 tionality constant  $\alpha_m$  was determined for each calendar month by means of a  
5 regression of the observed PET value for the Belgian part of the basin on the  
6 observed daily temperature, as in LB07. An elaborate description of the HBV  
7 model and its application to the Meuse basin can be found in Booij (2005).

### 8 **3 Bias correction of RCM data**

9 In LB07 the precipitation bias in the control simulation of RACMO-HC was  
10 discussed for the study area. Table 1 summarizes the performance of the used  
11 model configurations for the Meuse basin for the winter as well as the summer  
12 half-year. The observations for the 30-year period 1969-1998 were used as a  
13 reference. This period was also considered in LB07. All three model runs show  
14 a positive bias in the mean precipitation, in particular RAO-MPI. This bias  
15 is mainly related to that of the fraction  $f_{\text{wet}}$  of wet days ( $\geq 0.3$  mm), because  
16 the mean wet-day amount  $m_{\text{wet}}$  is fairly well reproduced. The left panel of Fig.  
17 2 shows the basin-average relative precipitation bias for each calendar month.  
18 RACMO-HC and RAO-HC have similar biases, whereas RAO-MPI has a  
19 much larger bias in the months July through October. The large positive bias  
20 in this part of the year is characteristic for control simulations driven by MPI  
21 for western Europe and is possibly related to a positive bias in the westerlies  
22 (van Ulden et al., 2007). Furthermore, the coefficient of variation of daily  
23 precipitation ( $\text{CV}_1$ ) is too low in all RCM runs. This is also the case for the  
24 CV of the 10-day precipitation amounts (not shown).

25 The first-order autocorrelation coefficient  $r_1$  in winter is overestimated by  
26 RAO-HC and slightly underestimated in the other two model configurations.  
27 In summer the same is found, though the differences between the models and  
28 the observations are somewhat larger.

29 A linear scaling of precipitation does not correct the underestimation of  $\text{CV}_1$   
30 or that of the multi-day CVs. It was shown by LB07 that this can have un-  
31 desirable effects on large quantiles of multi-day precipitation. Hence, such a  
32 correction is unsuited for any study of extreme precipitation and simulated  
33 discharge. A slightly more advanced nonlinear correction in the form

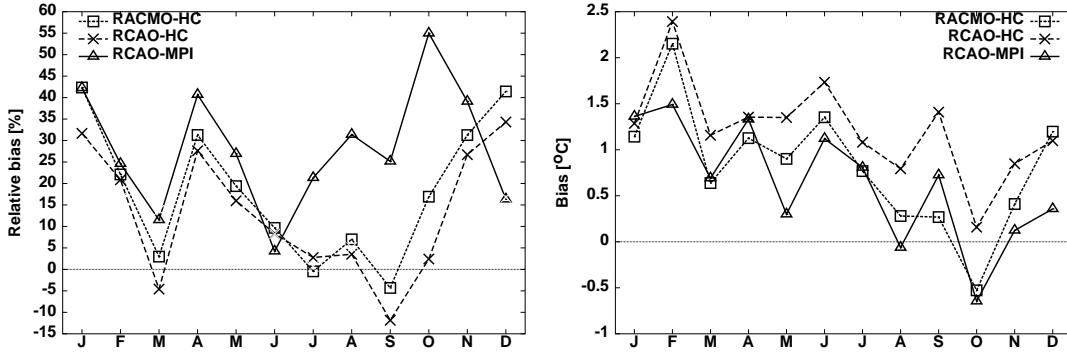


Fig. 2. Basin-average relative bias in the monthly precipitation (left) and the absolute bias in the mean monthly temperature (right) for the control simulations of RACMO-HC (squares), RCAO-HC (crosses) and RCAO-MPI (triangles) for the period 1961-1990. Biases are calculated with respect to the observed means for the period 1969-1998.

$$P^* = a P^b \quad (2)$$

1 was introduced in LB07 to correct the variability as well as the mean precipita-  
 2 tion. The seasonally and spatially varying (i.e. between subbasins) parameters  
 3  $a$  and  $b$  were determined for each interval of five calendar days in the year,  
 4 by considering days within a moving window of 65 days centered on the five-  
 5 day period of interest. For each window the values of  $a$  and  $b$  were chosen  
 6 such that the mean precipitation and the CV of 10-day precipitation amounts  
 7 ( $CV_{10}$ ) matched those of the corresponding days from the observed precipita-  
 8 tion. Figure 3 shows how the basin-average exponent  $b$  varies throughout the  
 9 year for all three control simulations. As observed for the biases in the mean  
 10 precipitation, there is a strong resemblance between the values of  $b$  for the  
 11 two HC-driven simulations. For the RCAO-MPI simulation the values of  $b$  are  
 12 considerably higher. In particular in the months September through November  
 13 (roughly between day 240 and day 330) the values of the exponent are rather  
 14 large. It was suspected that these large values were related to the positive bias  
 15 of  $f_{\text{wet}}$ . As an alternative  $f_{\text{wet}}$  was adjusted, prior to the nonlinear correction,  
 16 by subtracting a certain threshold amount and setting negative amounts to  
 17 zero. Though this resulted in smaller values of the exponent  $b$ , the reduction  
 18 was only marginal.

19 The right panel of Fig. 2 shows the absolute monthly temperature biases.  
 20 These were obtained by comparing the basin-average temperature calculated  
 21 from the grid boxes with the reference temperature for the basin, obtained  
 22 from station data of 11 stations using Thiessen interpolation. For the three  
 23 configurations the temperature biases are roughly of the same order, though  
 24 the bias of RCAO-HC, is on average larger than that of the other two model  
 25 configurations. The daily temperatures of the subbasins were corrected in the  
 26 same way as in LB07, involving a translation and a scaling which respectively

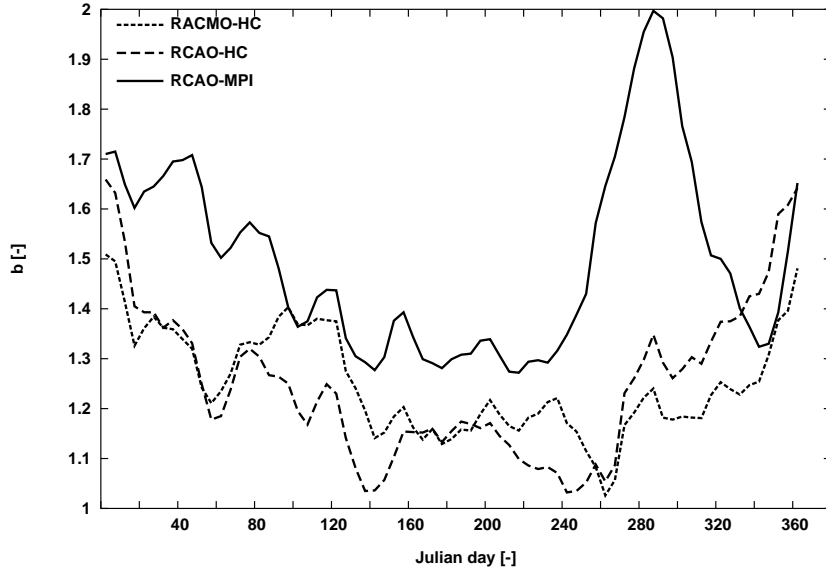


Fig. 3. Annual cycle of the area-averaged correction parameter  $b$  for RACMO-HC, RCAO-HC and RCAO-MPI.

Table 1

Performance of the three model configurations for the winter half-year (October-March) and the summer half-year (April-September). The mean daily amount, the coefficient of variation  $CV_1$ , the first order autocorrelation coefficient  $r_1$ , the fraction  $f_{\text{wet}}$  of wet days and the mean wet-day amount  $m_{\text{wet}}$  are area-weighted averages over all subbasins.

<b>Winter</b>	Observed	RACMO-HC	RCAO-HC	RCAO-MPI
Mean [mm/day]	2.77	3.49	3.25	3.58
$CV_1$	1.73	1.48	1.36	1.26
$r_1$	0.37	0.35	0.40	0.35
$f_{\text{wet}}$ [%]	55.79	67.91	70.29	75.60
$m_{\text{wet}}$ [mm/day]	4.94	5.10	4.60	4.72
<b>Summer</b>	Observed	RACMO-HC	RCAO-HC	RCAO-MPI
Mean [mm/day]	2.40	2.64	2.58	2.97
$CV_1$	1.81	1.69	1.69	1.54
$r_1$	0.27	0.25	0.31	0.22
$f_{\text{wet}}$ [%]	50.28	57.13	56.36	62.61
$m_{\text{wet}}$ [mm/day]	4.75	4.58	4.52	4.69

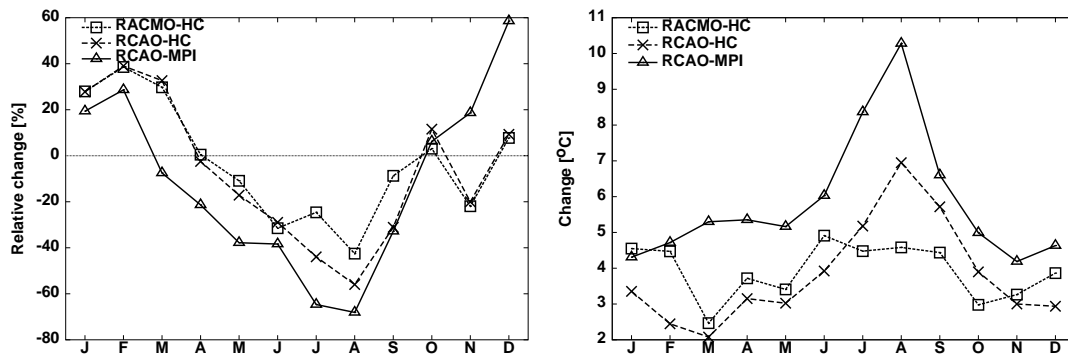


Fig. 4. Relative change in the monthly precipitation (left) and the absolute change in the monthly mean temperature (right), resulting from the A2 scenario, as projected by RACMO-HC, RCAO-HC and RCAO-MPI.

1 adjust the mean and the variability. The same translation and scale factor  
 2 were used for all subbasins, but these parameters were determined separately  
 3 for each 5-day interval in the year, again using a moving window of 65 calendar  
 4 days.

#### 5 4 Projected changes in temperature and precipitation

6 For each model configuration precipitation and temperature for the Meuse  
 7 basin in the A2-scenario run were compared with those in the control run. The  
 8 left panel of Fig. 4 displays the relative change of the mean precipitation. All  
 9 model configurations show an increase of winter precipitation and a decrease  
 10 in summer. The changes in RCAO-MPI are the largest in magnitude, ranging  
 11 from a decrease of about 70% in August to an increase of 60% in December.  
 12 The decrease in summer precipitation is accompanied by a strong decrease in  
 13 the number of wet days (30% to 50% in the summer months June, July and  
 14 August). In winter the change in precipitation frequency is small, but there  
 15 is a clear increase in the mean wet-day amounts. For December, January and  
 16 February, this increase ranges from 16% for the HC-driven runs up to 32% for  
 17 RCAO-MPI.

18 The right panel of Fig. 4 displays the change of the mean monthly temperature.  
 19 Throughout the entire year an increase is found in all model configurations.  
 20 The changes in both HC-driven runs do not differ much, except for August  
 21 and September, where RCAO-HC shows a considerably larger increase. This is  
 22 probably related to the drying-out of the soil, the effects of which can also be  
 23 seen in the precipitation in the summer months. In the RACMO model several  
 24 modifications of the soil scheme were made to prevent a feedback loop between  
 25 soil moisture and temperature. The soil depth was increased, the response of  
 26 the evapotranspiration to the available soil moisture was modified and the

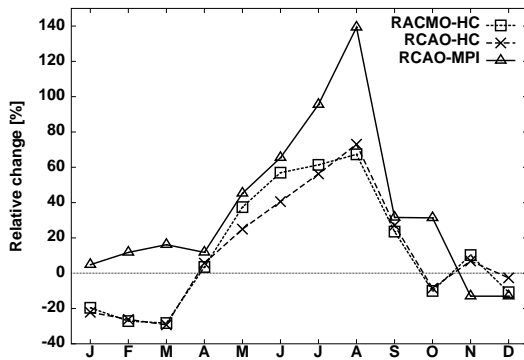


Fig. 5. Relative change of  $CV_{10}$  for each calendar month.

1 percolation of soil water to deeper layers was reduced. Furthermore, the cloud  
 2 scheme was altered to increase the cloud cover in summer (Lenderink et al.,  
 3 2003). In RCAO-MPI the change of the temperature in the summer months is  
 4 even larger than in RCAO-HC, especially in August, which shows an increase  
 5 of more than 10 degrees.

6 In Fig. 5 the relative change of  $CV_{10}$  is shown for all model configurations.  
 7 The close correspondence between both HC-driven runs, except for May and  
 8 June, suggests a strong influence of the driving GCM. For RACMO-HC and  
 9 RCAO-HC the change in winter is comparable to that found by Buishand and  
 10 Lenderink (2004) for the Rhine basin, using an RCM from the Hadley Centre  
 11 also driven by HC boundaries. They observed a decrease of 16% for the months  
 12 December, January and February. In summer the relative change in this study  
 13 is larger than the relative change found by Buishand and Lenderink (2004).

14 The change in  $CV_{10}$  can be understood from the changes in certain basic  
 15 statistical properties of the daily precipitation amounts. The value of  $CV_{10}$   
 16 is directly related to  $CV_1$  and the autocorrelation coefficients  $r_i$ :

$$CV_{10}^2 = \frac{CV_1^2}{10} \left( 1 + 2 \sum_{i=1}^9 r_i \frac{10-i}{10} \right) \quad (3)$$

17 For  $CV_1$  Räisänen (2002) derived

$$CV_1^2 = \left( \frac{CV_{\text{wet}}^2 + 1}{f_{\text{wet}}} - 1 \right) \quad (4)$$

18 where  $CV_{\text{wet}}$  is the CV of the wet-day precipitation amounts. From these  
 19 equations it can be seen that  $CV_{10}$  decreases with the number of wet days and  
 20 increases with  $CV_{\text{wet}}$  and the autocorrelation coefficients. Figure 6 shows the  
 21 relative change of  $f_{\text{wet}}$  and  $CV_{\text{wet}}$  (left panel) and the relative change of  $CV_1$ ,  
 22  $CV_{10}$  and  $r_{123} = r_1 + r_2 + r_3$  (right panel) for the RACMO-HC run. From the

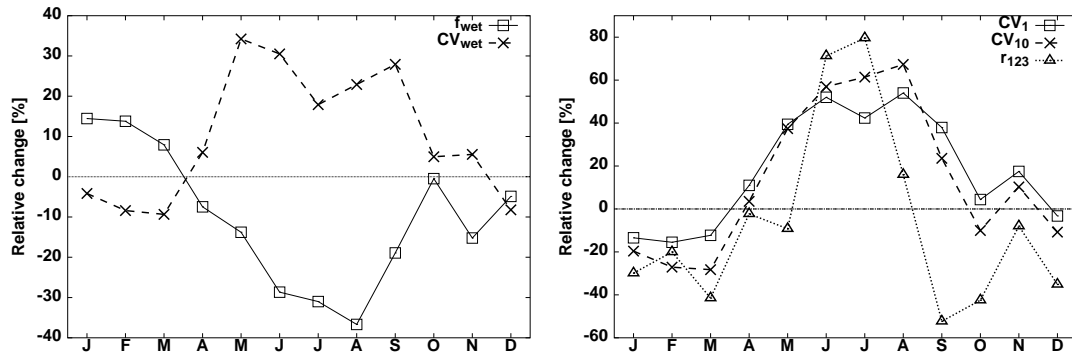


Fig. 6. Basin-average relative change of  $f_{\text{wet}}$  and  $CV_{\text{wet}}$  for RACMO-HC (left panel) and the corresponding basin-average relative change of  $CV_1$ ,  $CV_{10}$  and the sum of the first three autocorrelation coefficients  $r_{123}$  (right panel).

1 latter it is seen that the direction of change of the autocorrelation coefficients,  
 2 determines whether or not the change of  $CV_{10}$  exceeds that of  $CV_1$ . In January,  
 3 February and March  $f_{\text{wet}}$  increases and  $CV_{\text{wet}}$  decreases, resulting in a decrease  
 4 of  $CV_1$ . This effect is accompanied by a decrease of the autocorrelation, leading  
 5 to a larger decrease for  $CV_{10}$  than for  $CV_1$ . The rather large increase of  $CV_{10}$   
 6 for the months June, August and September ( $\approx 60\%$ ) can be attributed to an  
 7 increase of  $CV_{\text{wet}}$  and the strength of the autocorrelation in combination with  
 8 a decrease of  $f_{\text{wet}}$ .

9 The seasonal changes of  $f_{\text{wet}}$ ,  $CV_{\text{wet}}$  and the autocorrelation in RAO-HC are  
 10 similar to those in RACMO-HC. The results for RAO-MPI for the winter  
 11 half-year are, however, quite different. There is a slight increase in  $CV_{10}$  ( $\approx$   
 12  $5\%$ ), mainly due to an increase of  $CV_{\text{wet}}$ .

## 13 5 Simulated changes in precipitation extremes

14 The Nearest-Neighbour resampling algorithm explained earlier was applied to  
 15 the RCM control runs to simultaneously generate daily sequences of precipi-  
 16 tation and temperature for the 15 subbasins, each with a length of 9000 years.  
 17 The corrections discussed earlier were used to adjust the mean and  $CV_{10}$  of  
 18 modelled precipitation amounts and the mean and standard deviation of the  
 19 daily temperatures. This procedure was repeated for the A2-scenario runs, us-  
 20 ing the same bias corrections. In this section the distribution of the simulated  
 21 10-day maxima of basin-average precipitation for the winter half-year (flood-  
 22 ing season) are discussed. The three panels A, B and C in Fig. 7 compare the  
 23 Gumbel plots of these maxima in the control run and the A2-scenario run for  
 24 each model configuration.

25 For RACMO-HC (panel A) a slight decrease is seen for return periods longer

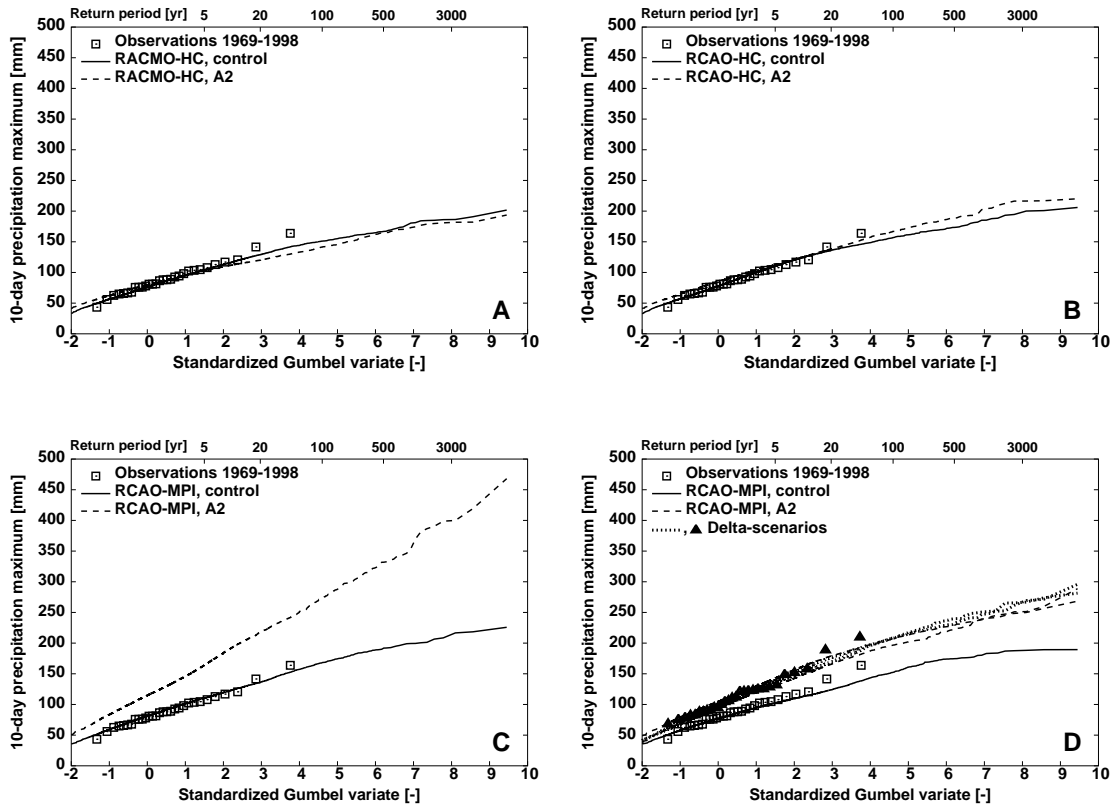


Fig. 7. Gumbel plots for the 10-day winter maxima of basin-average precipitation obtained after resampling and bias correction. Panels A, B and C show the results for the three model configurations: RACMO-HC, RCAO-HC and RCAO-MPI. Panel D shows the effect of limiting the bias correction on the resampled A2-scenario run from RCAO-MPI (dashed) and the ‘delta’ scenarios, obtained by applying the relative changes found in RCAO-MPI to various control runs (dotted) and the observations (triangles).

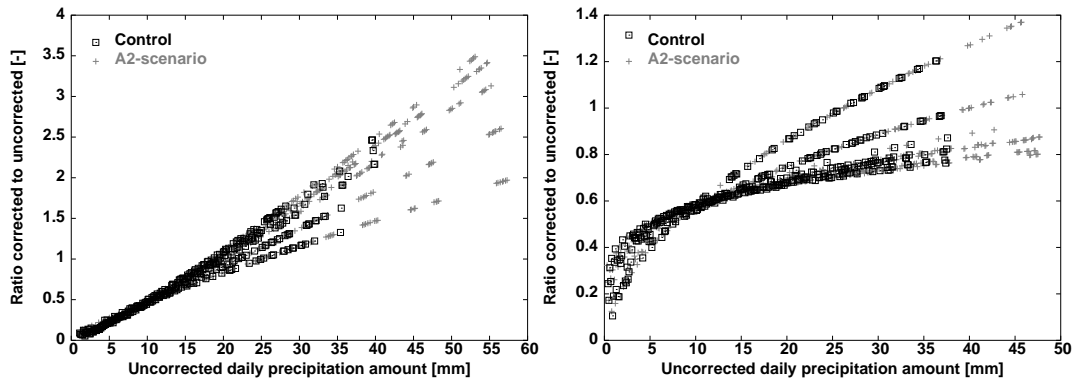


Fig. 8. Ratio between the corrected and uncorrected precipitation amounts for individual wet days in October (left) and December (right) in RCAO-MPI for the Ourthe subbasin (1588 km<sup>2</sup>). The results for both the A2-scenario run and control run are shown. The days falling within the same 5-day period in the year (and thus having the same transformation parameters) form a curve in the plot.

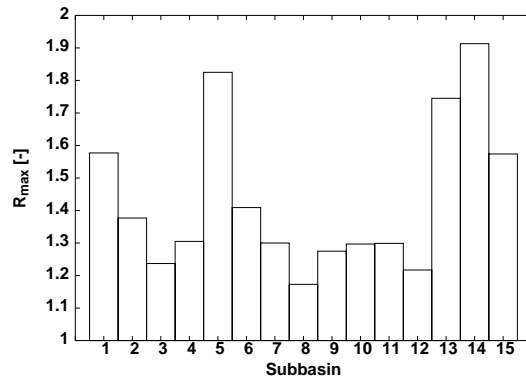


Fig. 9. The upper bound of the ratio between the corrected and uncorrected daily precipitation amount  $R_{\max}$  for each subbasin. The numbers are assigned to the subbasin in downstream order. Subbasins 1 through 4 are located in France, subbasins 5 through 15 in Belgium.

1 than five years. The change of the highest quantiles of the distribution is less  
 2 than 10 mm. The effect of the increase in the mean precipitation is coun-  
 3 terbalanced here by the decrease of  $CV_{10}$ , shown in Fig. 5. Describing the  
 4 distributions of the 10-day precipitation amounts by a square-root-normal dis-  
 5 tribution, it is demonstrated in Appendix A that the changes in the mean and  
 6  $CV_{10}$  can account for the changes in the extreme value distribution. Although  
 7 a slight increase in the most extreme quantiles of 10-day precipitation is seen  
 8 for RCAO-HC (panel B), the changes are comparable to those of RACMO-HC.

9 The results found for RCAO-MPI (panel C) are, however, strikingly different.  
 10 The most extreme quantiles are roughly doubled. This large increase is most  
 11 likely related to the nonlinear bias correction. Figure 8 presents the ratios be-  
 12 tween the corrected and uncorrected daily precipitation amounts in the months  
 13 of October and December for the Ourthe subbasin. From the left panel it can  
 14 be seen that in October the highest values in the A2-scenario run are multi-  
 15 plied by more than a factor of three, due to the large correction exponent  $b$  in  
 16 Eqn. 2 for that month (see Fig. 3). This results in daily precipitation amounts  
 17 exceeding 160 mm. In some occasions, two such values occurred within a short  
 18 time span, leading to extremely large 10-day amounts. For December (right  
 19 panel) the correction ratios are all below 1.5.

20 To limit the effect of the nonlinearity of the bias correction on large daily  
 21 precipitation amounts, a modification was made to restrict the ratio between  
 22 corrected and uncorrected daily precipitation amounts to an upper bound  
 23  $R_{\max}$ . For each period of five calendar days the ratio between the average of  
 24 the 20 largest daily precipitation amounts within a centered 65-day window  
 25 (similar to that used for the determination of  $a$  and  $b$ ) from the control run  
 26 data and the observations was calculated.  $R_{\max}$  was then set equal to the  
 27 maximum of these ratios over the year. This procedure was performed for  
 28 each subbasin separately. From Fig. 9 it can be seen that  $R_{\max}$  varies between

1 1.2 and 1.9.

2 The effect of the limited correction is shown in panel D of Fig. 7. For the  
3 control run, the quantiles of the 10-day winter maxima are somewhat lower  
4 than if no restriction were applied (Panel C). The agreement with the ob-  
5 served quantiles is, however, still satisfactory. Limiting the bias correction has  
6 a substantial effect on the extreme quantiles of the A2-scenario run. Because  
7 the changes in  $CV_{10}$  for the RCAO-MPI runs were found to be small in win-  
8 ter (see Fig. 5), it was expected that a ‘delta’ scenario, i.e. scaling the daily  
9 precipitation amounts of the control run by a seasonally varying factor (which  
10 represents the relative changes in the mean precipitation) may sufficiently de-  
11 scribe the changes of the winter extremes. Therefore, the changes in the mean  
12 precipitation in RCAO-MPI were applied to the observations and the control  
13 runs from all three model configurations. Panel D of Fig. 7 shows that the  
14 10-day winter maxima in the resulting delta-scenarios resemble those from  
15 the A2-scenario run with a limited nonlinear bias correction. This result gives  
16 confidence that the limited nonlinear bias correction leads to realistic extreme  
17 quantiles of 10-day precipitation for the A2 scenario. Therefore, the RCAO-  
18 MPI simulation with the limited nonlinear bias correction is used further for  
19 the estimation of the changes in flood quantiles.

## 20 **6 Estimation of changes in flood quantiles**

21 The bias-corrected resampled series of daily precipitation and temperature  
22 discussed earlier, were used to drive hydrological simulations with the HBV  
23 rainfall-runoff model. Figure 10 shows the Gumbel plots of the simulated win-  
24 ter maxima of daily discharge at Borgharen.

25 The flood quantiles obtained from RACMO-HC (panel A) and RCAO-HC  
26 (panel B) show roughly the same response to the A2 scenario. For both model  
27 configurations a slight decrease is seen for intermediate return periods, whereas  
28 quantiles for the longest return periods tend to increase, in particular for  
29 RACMO-HC. For RCAO-MPI (panel C) the response of flood quantiles to  
30 the A2 scenario is much larger than for the HC-driven simulations. This is  
31 consistent with the change of the 10-day precipitation maxima. These results  
32 suggest that, at least for the winter half-year, the change of flood quantiles  
33 is more sensitive to the change of large scale characteristics, produced by the  
34 GCM, than to local effects produced by the RCM.

35 Figure 11 displays the relative change of the flood quantiles as a function  
36 of the standardized Gumbel variate, showing more clearly the different re-  
37 sponses of the three model configurations to the A2 scenario. The changes for  
38 the RACMO-HC and RCAO-HC simulations are slightly different from those

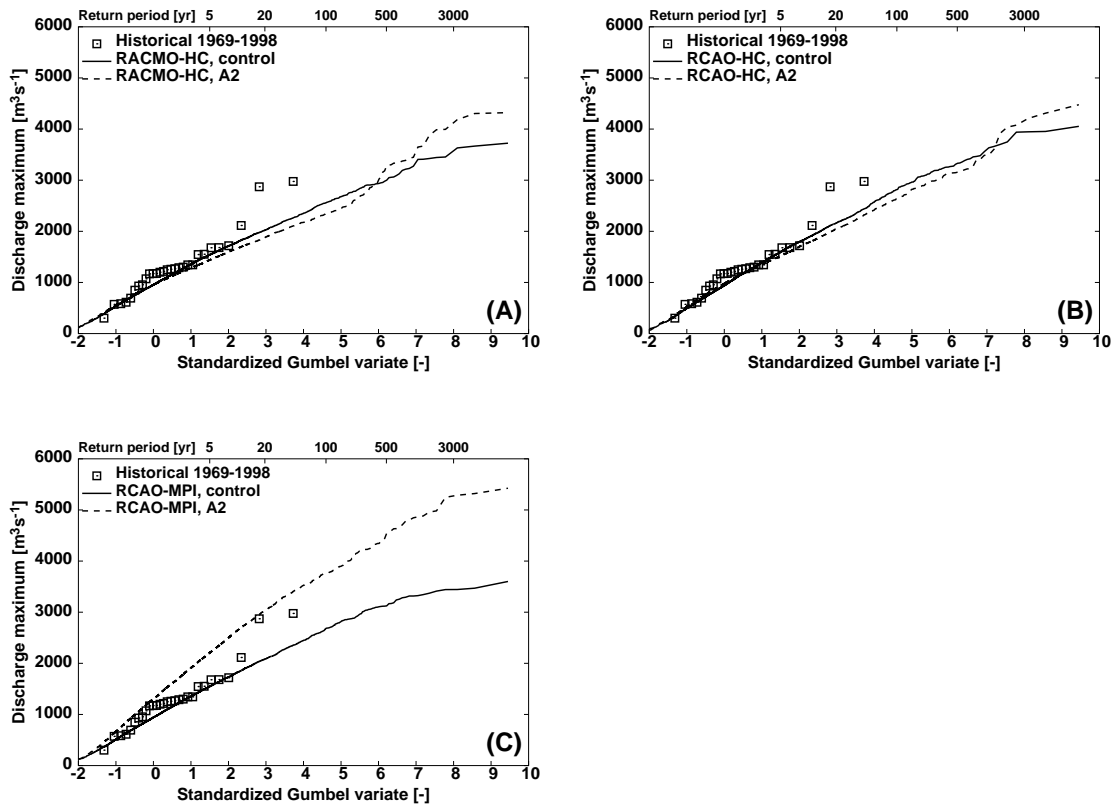


Fig. 10. Gumbel plots for the maxima of daily discharge in the winter half-year for the three model configurations RACMO-HC, RCAO-HC and RCAO-MPI, the latter with the limited bias correction.

1 found by Buishand and Lenderink (2004) and Lenderink et al. (2006) for the  
 2 flood quantiles of the river Rhine. They found a rise of 10% in the 100-year  
 3 flood. This increase is, however, less than the increase of the mean winter  
 4 discharge, which is most likely related to the decrease of the CV of 10-day  
 5 precipitation amounts in winter in the HC-driven runs mentioned earlier. For  
 6 RCAO-MPI the relative change is between 35% and 55% over virtually the  
 7 entire range of return periods.

8 In order to explore the influence of the bias correction on the changes of  
 9 the flood quantiles, the HBV simulations were repeated with the uncorrected  
 10 resampled data from RACMO-HC and RCAO-MPI. The relative changes in  
 11 the flood quantiles are compared in Fig. 12. For the RACMO-HC simulations  
 12 (left panel) the relative change of flood quantiles is only slightly affected by the  
 13 bias correction up to a return period of 100 years. For return periods beyond  
 14 500 years, the flood quantiles from the corrected data increase by about 15%,  
 15 whereas those from the uncorrected data decrease by approximately the same  
 16 amount. For the RCAO-MPI simulations the relative change obtained from  
 17 uncorrected data is systematically lower than that obtained *with* the nonlinear  
 18 bias correction. These results confirm the need for bias-corrected precipitation  
 19 to estimate the changes of flood quantiles for long return periods.

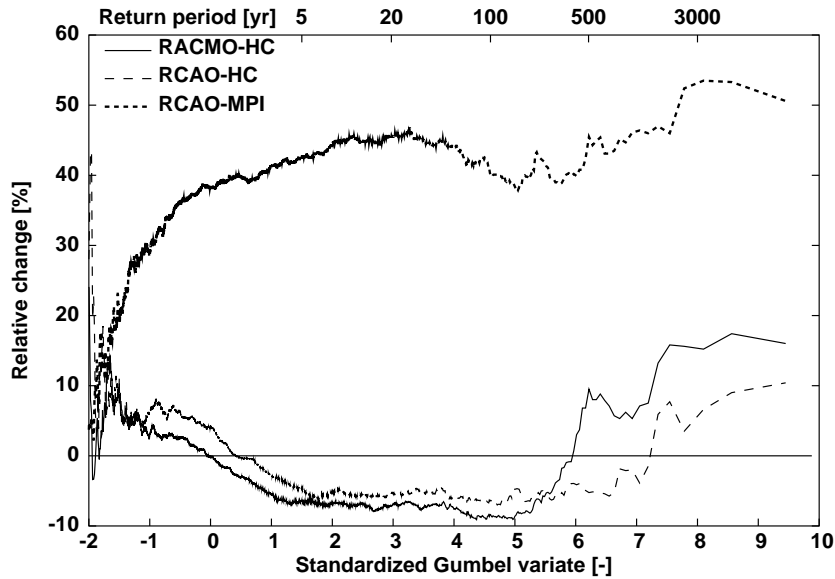


Fig. 11. Relative change of the flood quantiles as a function of the standardized Gumbel variate for the three model configurations.

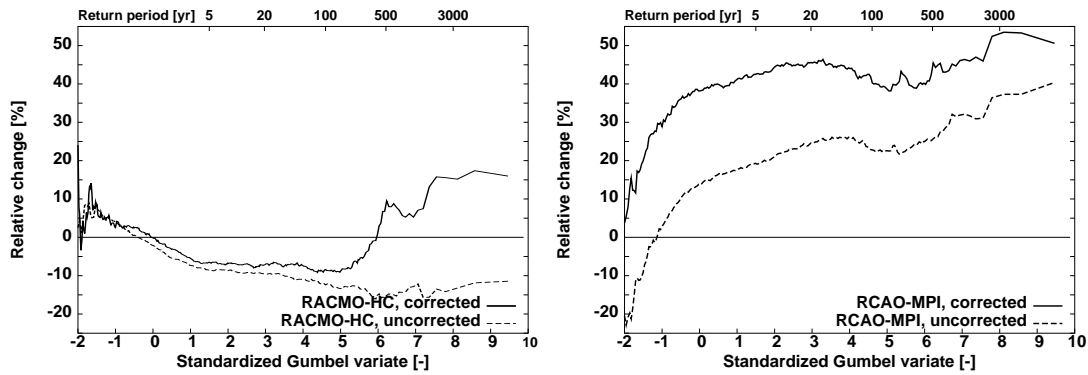


Fig. 12. Influence of the nonlinear bias correction on the relative change of the simulated flood quantiles for RACMO-HC (left panel) and RCAO-MPI (right panel).

## 1 7 Conclusion

2 Daily precipitation and temperature from three RCM simulations (RACMO-  
 3 HC, RCAO-HC and RCAO-MPI) were used to estimate the changes in flood  
 4 quantiles of the river Meuse. For each model configuration, two 9000-year se-  
 5 quences were generated by resampling from the control run (1961-1990) and  
 6 the A2-scenario run (2071-2100). These sequences were corrected for differ-  
 7 ences in the mean and variability between the control run and observed cli-  
 8 mate. The HBV rainfall-runoff model was used to simulate the daily discharges  
 9 at the gauging station Borgharen. The changes in the flood quantiles for the  
 10 winter half-year were studied.

11 A substantial difference was found between the changes in flood quantiles from

1 the two HC-driven simulations and those obtained from the RCAO-MPI simu-  
2 lations. In the HC-driven simulations there was little change in both the quan-  
3 tiles of extreme 10-day precipitation and the flood quantiles, despite a clear  
4 increase in the mean winter precipitation (Fig. 4). This could be explained  
5 by the fact that the increase in the mean precipitation was counteracted by  
6 a decrease in  $CV_{10}$ . By contrast, in the RCAO-MPI simulations there was  
7 little change in the  $CV_{10}$ . Mainly due to the increase of the mean precipita-  
8 tion amounts the quantiles of the 10-day precipitation maxima and the daily  
9 discharges increase by about 50%.

10 Apart from the change in the mean winter precipitation, the change in the  
11 CV of the multi-day precipitation amounts is thus an important indicator of  
12 the changes in flood quantiles. Little is known about the change of the CV in  
13 RCM simulations. For GCM simulations an extensive study was carried out by  
14 Räisänen (2002). In that study 19 atmosphere-ocean GCMs were considered,  
15 all forced with an increase in the atmospheric  $CO_2$  concentration of  $1\% \text{ yr}^{-1}$ .  
16 For most areas of the world an increase in the CV of monthly precipitation was  
17 found. However, for the high northern latitudes ( $50^\circ\text{N}$  and higher) a decrease  
18 was observed for autumn and winter. This decrease was associated with a  
19 relatively large increase in the mean monthly precipitation. Similar results  
20 have been found for the change in the CV of seasonal precipitation (Rowell,  
21 2005; Giorgi and Bi, 2005). The change in the CV of multi-day precipitation  
22 is entirely determined by the changes in the frequency of wet days, the CV of  
23 the wet-day precipitation and the autocorrelation of daily precipitation. For  
24 the decrease of  $CV_{10}$  in the HC-driven simulations, all these factors had some  
25 influence.

26 It was found that the relative change of simulated flood quantiles depended  
27 on whether or not a bias correction was used, in particular for the RCAO-MPI  
28 simulation. LB07 already showed that a nonlinear bias correction, adjusting  
29 the relative variability of multi-day precipitation amounts, is essential for a  
30 realistic simulation of extreme flood quantiles. However, for the RCAO-MPI  
31 simulation the correction had to be restricted to avoid the occurrence of un-  
32 realistically large daily precipitation amounts.

33 It should be noted that the uncertainty in the change of the flood quantiles  
34 increases with the return period. Part of the uncertainty can be reduced by  
35 prolonging the meteorological sequences in the resampling stage. However, the  
36 uncertainty related to the limited length of the RCM runs remains. Since there  
37 is only one 30-year realization for each model experiment, this uncertainty is  
38 difficult to quantify. Furthermore, it is not clear whether the linear relation  
39 between PET and temperature derived for the current climate, is still valid in  
40 a changed climate or should be modified. However, it was shown by Lenderink  
41 et al. (2006) that the influence of assumptions regarding the potential evap-  
42 oration on extreme discharges are very small compared to other sources of

1 uncertainty.

2 Summarizing, this study shows that meaningful estimates of changes in ex-  
3 treme flood quantiles can be obtained from the daily output of RCM exper-  
4 iments. Apart from the change in the mean precipitation, the change in the  
5 CV of 10-day precipitation amounts emerged to be important for the Meuse  
6 basin. These changes are controlled strongly by the driving GCM. Finally,  
7 bias corrections of precipitation can have a strong influence on the estimated  
8 changes of flood quantiles and should therefore be applied with care.

9 **Acknowledgements** The station records and subbasin data for the Belgian  
10 part of the Meuse basin were kindly provided by the Royal Meteorological  
11 Institute of Belgium. The French station data were made available by Météo  
12 France. The RCM data from the PRUDENCE project were generously pro-  
13 vided by Bart van den Hurk, whose useful comments also helped to improve  
14 this paper.

## 15 **References**

- 16 Booiij, M. J., 2002. Appropriate modelling of climate change impacts on river  
17 flooding. PhD thesis, University of Twente, Enschede.
- 18 Booiij, M. J., 2005. Impact of climate change on river flooding assessed with  
19 different spatial model resolutions. *Journal of Hydrology* 303, 176–198.
- 20 Buishand, T. A., Lenderink, G., 2004. Estimation of future discharges of  
21 the river Rhine in the SWURVE project. Technical report TR-273, Royal  
22 Netherlands Meteorological Institute (KNMI), De Bilt.
- 23 Christensen, J. H., Christensen, O. B., 2007. A summary of the PRUDENCE  
24 model projections of changes in the European climate by the end of this  
25 century. *Climatic Change* in press.
- 26 de Wit, M. J. M., van den Hurk, B., Warmerdam, P. M. M., Torfs, P. J.  
27 J. F., Roulin, E., van Deursen, W. P. A., 2006. Impact of climate change on  
28 low-flows in the river Meuse. *Climatic Change* in press.
- 29 Giorgi, F., Bi, X., 2005. Regional changes in surface climate interannual vari-  
30 ability for the 21st century from ensembles of global model simulations.  
31 *Geophysical Research Letters* 32, L13701, doi:10.1029/2005GL023002.
- 32 Grabs, W. (ed), 1997. Impact of climate change on hydrological regimes and  
33 water resources management in the Rhine basin. CHR Report I-16, Secre-  
34 tariat of the International Commission for the Rhine basin (CHR), Lelystad.
- 35 Hershfield, D. M., 1961. Rainfall Frequency Atlas of the United States. Tech-  
36 nical Paper 40, U.S. Department of Commerce, Weather Bureau.
- 37 Jacob, D., Co-authors, 2007. An inter-comparison of regional climate models  
38 for Europe: Design of the experiments and model performance. *J. Climate*  
39 in press.
- 40 Jones, R., Murphy, J., Hassel, D., Taylor, R., 2001. Ensemble mean changes in

- 1 the simulation of the European climate of 2071-2100 using the new Hadley  
2 Centre regional modelling system HadAM3H/HadRM3H. Tech. Rep. March  
3 2001, p 19, Hadley Centre of the UK Met Office type = Hadley Centre  
4 Report.
- 5 Katz, R. W., 1999. Power transformed time series. *Environmetrics* 10, 301–  
6 307.
- 7 Kay, A. L., Jones, R. G., Reynard, N. S., 2006. RCM rainfall for UK flood  
8 frequency estimation. II Climate change results. *Journal of Hydrology* 318,  
9 163–172.
- 10 Kwadijk, J., Rotmans, J., 1995. The impact of climate change on the river  
11 Rhine: A scenario study. *Climatic Change* 30, 397–426.
- 12 Leadbetter, M. R., Lindgren, G., Rootzén, H., 1983. *Extremes and related*  
13 *properties of random sequences and processes*. Springer-Verlag, New York.
- 14 Leander, R., Buishand, T. A., 2007. Resampling of regional climate model  
15 output for the simulation of extreme river flows. *Journal of Hydrology* 332,  
16 487–496.
- 17 Leander, R., Buishand, T. A., Aalders, P., de Wit, M. J. M., 2005. Estimation  
18 of extreme floods of the river Meuse using a stochastic weather generator  
19 and a rainfall-runoff model. *Hydrological Sciences Journal* 50, 1089–1103.
- 20 Lenderink, G., Buishand, T. A., van Deursen, W., 2006. Estimates of future  
21 discharges of the river Rhine using two scenario methodologies: direct versus  
22 delta approach. *Hydrology and Earth System Sciences* in press.
- 23 Lenderink, G., van den Hurk, B. J. J. M., van Meijgaard, E., van Ulden, A. P.,  
24 Cuijpers, H., 2003. Simulation of present-day climate in RACMO2: first re-  
25 sults and model developments. Technical Report TR-252, Royal Netherlands  
26 Meteorological Institute (KNMI), De Bilt.
- 27 Lindström, G., Johansson, B., Persson, M., Gardelin, M., Bergström, S., 1997.  
28 Development and test of the distributed HBV-96 hydrological model. *Jour-  
29 nal of Hydrology* 201, 272–288.
- 30 Middelkoop, H. (ed), 2000. The impact of climate change on the river Rhine  
31 and the implications for water management in the Netherlands. Summary of  
32 the NRP project 952210. RIZA Report 2000.010, Institute for Inland Water  
33 Management and Waste Water Treatment (RIZA), Lelystad.
- 34 Räisänen, J., 2002. CO<sub>2</sub>-induced changes in interannual temperature and pre-  
35 cipitation variability in 19 CMIP experiments. *Journal of Climate* 15, 2395–  
36 2411.
- 37 Räisänen, J., Hansson, U., Ullerstig, A., Döscher, R., Graham, L. P., Jones,  
38 C., Meier, H. E. M., Samuelsson, P., Willén, U., 2004. European climate in  
39 the late twenty-first century: regional simulations with two driving global  
40 models and two forcing scenarios. *Climate Dynamics* 22, 13–31.
- 41 Rajagopalan, B., Lall, U., 1999. A k-nearest-neighbor simulator for daily pre-  
42 cipitation and other variables. *Water Resources Research* 35, 3089–3101.
- 43 Roeckner, E., Bengtsson, L., Feichter, J., Lelieveld, J., Rodhe, H., 1999. Tran-  
44 sient climate change simulations with a coupled atmosphere-ocean GCM  
45 including the tropospheric sulfur cycle. *Journal of Climate* 12, 3004–3032.

- 1 Rowell, D. P., 2005. A scenario of European climate change for the late twenty-  
2 first century: seasonal means and interannual variability. *Climate Dynamics*  
3 25, 837–849.
- 4 Shabalova, M. V., van Deursen, W. P. A., Buishand, T. A., 2003. Assessing  
5 future discharge of the river Rhine using regional climate model integrations  
6 and a hydrological model. *Climate Research* 23, 233–246.
- 7 Smith, R. L., 1990. Extreme value theory. In: Ledermann, W. et al. (Eds.),  
8 *Handbook of Applicable Mathematics, Supplement*. Wiley, Chichester, pp.  
9 437-472.
- 10 Tu, M., 2006. Assessment of the effects of climate variability and land use  
11 change on the hydrology of the Meuse river basin. PhD thesis, UNESCO-  
12 IHE, Delft, the Netherlands.
- 13 van Ulden, A. P., Lenderink, G., van den Hurk, B. J. J. M., van Meijgaard,  
14 E., 2007. Circulation statistics and climate change in central Europe: PRU-  
15 DENCE simulations and observations. *Climatic Change in press*.

## 1 A Approximation of the extreme value distribution

This appendix investigates whether the change in the quantiles of the extreme 10-day precipitation amounts in the RACMO-HC simulations can be explained by the changes in the mean and CV alone. The distribution of the 10-day precipitation amounts  $P_{10}$  can satisfactorily be described by the square-root-normal distribution, i.e.  $X = \sqrt{P_{10}}$  is normally distributed with mean  $\mu_x$  and standard deviation  $\sigma_x$ . These two parameters determine the mean  $\mu_p$  and standard deviation  $\sigma_p$  of  $P_{10}$  (Katz, 1999):

$$\mu_p = \mu_x^2 + \sigma_x^2 \quad \text{and} \quad \sigma_p^2 = 2\sigma_x^2 (\sigma_x^2 + 2\mu_x^2) \quad (\text{A.1})$$

2 Here these relations are used to derive  $\mu_x$  and  $\sigma_x$  from  $\mu_p$  and  $\sigma_p$ :

$$\sigma_x^2 = \mu_p - \sqrt{\mu_p^2 - \frac{1}{2}\sigma_p^2} \quad \text{and} \quad \mu_x^2 = \sqrt{\mu_p^2 - \frac{1}{2}\sigma_p^2} \quad (\text{A.2})$$

3 Figure A.1 displays the empirical quantiles of 10-day precipitation amounts,  
 4 based on their plotting positions, versus the theoretical quantiles of the gamma  
 5 and square-root-normal distributions, with the same mean and standard de-  
 6 viation as the data. These quantile-quantile plots show that the square-root-  
 7 normal distribution performs better than the gamma distribution. The latter  
 8 clearly overestimates the upper quantiles of  $P_{10}$ .

9 The distribution of the 10-day winter maxima can be derived from the distribu-  
 10 tion of  $P_{10}$ ,  $F(x) = P(P_{10} \leq x)$ , using extreme-value theory. Let  $M_n$  be the max-  
 11 imum of the 10-day precipitation amounts in  $n$  subsequent, non-overlapping  
 12 10-day periods. Assuming independence between the precipitation amounts,  
 13 the distribution of  $M_n$  is given by (Leadbetter et al., 1983):

$$H(x) \equiv \text{Prob}(M_n \leq x) = \{F(x)\}^n \sim \exp\{-n[1 - F(x)]\} \quad (\text{A.3})$$

14 This distribution can be approximated by a GEV distribution (Smith, 1990):

$$H(x) \equiv \text{Prob}(M_n \leq x) = \exp\left\{-[1 - \theta(x - \mu)/\sigma]^{1/\theta}\right\} \quad (\text{A.4})$$

15 The parameters  $\mu$ ,  $\sigma$  and  $\theta$  of  $H$  depend on  $n$ . The location parameter  $\mu$  is  
 16 obtained as the  $1/n$  upper quantile of  $F$ , i.e.

$$1 - F(\mu) = 1/n \quad (\text{A.5})$$

Fig. A.1. Quantile-quantile plots of the basin-average 10-day precipitation amounts in the winter half-year for the control run (left) and the A2-scenario run (right) of RACMO-HC, assuming different distributions. The bias-corrected precipitation was used.

- 1 Subsequently, the scale parameter  $\sigma$  and the shape parameter  $\theta$  are calculated  
 2 using the first and second derivatives  $F'$  and  $F''$  of  $F$  in  $\mu$ :

$$\sigma = \frac{1}{n} \frac{1}{F'(\mu)} \quad \text{and} \quad \theta = \sigma \frac{F''(\mu)}{F'(\mu)} + 1 \quad (\text{A.6})$$

- 3 This approximation is known as the penultimate distribution.  
 4 Since the winter half-year is considered here, a value of 18.5 was chosen for  $n$ .  
 5 Because  $z = (\sqrt{P_{10}} - \mu_x) / \sigma_x$  is assumed to be standard-normally distributed  
 6 the solution of Eqn. A.5 is given by

$$\mu = \left( \mu_x + \sigma_x \Phi^{-1}(1/n) \right)^2 \quad (\text{A.7})$$

where  $\Phi^{-1}$  is the inverse of the standard normal distribution function. The probability density  $F'$  and its derivative  $F''$  in  $\mu$ , which are required to calculate the scale parameter  $\sigma$  and the shape parameter  $\theta$ , are given by

$$F'(\mu) = \frac{1}{2\sigma_x \sqrt{\mu}} \varphi(z) \quad (\text{A.8})$$

and

$$F''(\mu) = -\frac{1}{4\mu\sigma_x} \varphi(z) \left( \frac{1}{\sqrt{\mu}} + \frac{z}{\sigma_x} \right) \quad (\text{A.9})$$

1 where  $\varphi$  denotes the standard normal density.

2 The 10-day precipitation maxima considered in this paper (Fig. 5) refer to  
3 overlapping 10-day periods. These maxima are generally larger than those for  
4 consecutive 10-day periods. To account for this, the location parameter  $\mu$  and  
5 the scale parameter  $\sigma$  were multiplied by 1.13, which implies that the quantiles  
6 of the distribution of  $M_n$  change with the same factor. The factor 1.13 is due  
7 to Hershfield (1961). It has been used to adjust the quantiles of clock-hour  
8 and 1-day maxima to the corresponding quantiles of sliding 60-minute and  
9 24-hour maxima respectively.

10 For the the 10-day precipitation amounts in winter from the control run of  
11 RACMO-HC Fig. A.2 compares the Gumbel plots of the 30-year run and  
12 the 9000-year resampled series with the penultimate approximation. For the  
13 penultimate approximation,  $\mu = 79.4$  mm,  $\sigma = 21.2$  mm and  $\theta = 0.0755$ .  
14 It is seen that this GEV distribution slightly overestimates the quantiles of  
15 the resampled maxima, though there is a good agreement with those of the  
16 30-year RCM run.

17 Figure A.3 shows the relative change of the quantiles of the 10-day winter  
18 maxima. The change derived from the penultimate approximation roughly  
19 agrees with that found from the resampled sequences. This indicates that the  
20 changes of the mean and  $CV_{10}$  can account for the change of the quantiles of  
21 the maxima in winter.

Fig. A.2. Penultimate approximation of the distributions of extreme 10-day basin-average precipitation totals for the winter half-year (dashed), compared with the empirical quantiles from a 9000-year resampled series (solid) and those of the 30-year RCM control run (squares).

Fig. A.3. Change in the quantiles of the 10-day winter maxima of basin-average precipitation, extracted from the bias-corrected 30-year control run and A2-scenario run of RACMO-HC (boxes) and from the corresponding 9000-year resampled sequences (solid) and penultimate approximations (dashed) derived from these runs.